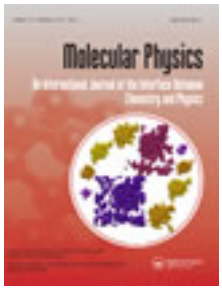

Molecular Physics: An International Journal at the Interface Between Chemistry and Physics
Publication details, including instructions for authors and subscription information:
http://www.tandfonline.com/loi/tmph20

On the gas-liquid phase separation and the self-assembly of charged soft dumbbells

Simone Dussi[ab], Lorenzo Rovigatti[a] & Francesco Sciortino[ac]

[a] Dipartimento di Fisica, Sapienza Università di Roma, Roma, Italy

[b] Soft Condensed Matter, Debye Institute for Nanomaterials Science, Utrecht University, Utrecht, The Netherlands

[c] CNR-ISC, Sapienza Università di Roma, Roma, Italy

Accepted author version posted online: 28 Aug 2013.Published online: 25 Sep 2013.

To cite this article: Simone Dussi, Lorenzo Rovigatti & Francesco Sciortino (2013) On the gas-liquid phase separation and the self-assembly of charged soft dumbbells, Molecular Physics: An International Journal at the Interface Between Chemistry and Physics, 111:22-23, 3608-3617, DOI: 10.1080/00268976.2013.838315

To link to this article: http://dx.doi.org/10.1080/00268976.2013.838315

Molecular Physics, 2013
Vol. 111, Nos. 22–23, 3608–3617, http://dx.doi.org/10.1080/00268976.2013.838315

INVITED ARTICLE

On the gas–liquid phase separation and the self-assembly of charged soft dumbbells

Simone Dussi[a,b,*], Lorenzo Rovigatti[a] and Francesco Sciortino[a,c]

[a]*Dipartimento di Fisica, Sapienza Università di Roma, Roma, Italy;* [b]*Soft Condensed Matter, Debye Institute for Nanomaterials Science, Utrecht University, Utrecht, The Netherlands;* [c]*CNR-ISC, Sapienza Università di Roma, Roma, Italy*

(*Received 27 June 2013; accepted 21 August 2013*)

We investigate the phase behaviour of charged soft dumbbells, particles composed of two soft but oppositely charged sites, as a function of the separation between the sites. Through successive umbrella sampling Monte Carlo simulations, we evaluate the equilibrium particle density of states. For elongated dumbbells, we recover the expected critical behaviour. However, reducing the elongation we are unable to locate the gas–liquid critical point in the accessible region of temperature and density. Correspondingly, the self-assembly of the particles in ring structures becomes dominant with respect to the formation of chain-like structures. Our results enrich the debate on the competition between self-assembly and phase separation and contribute to the long-standing dilemma about the putative gas–liquid criticality in dipolar fluids.

Keywords: soft matter; charged dumbbells; gas–liquid separation; self-assembly; Monte Carlo simulation

1. Introduction

Dipolar fluids are systems composed of particles carrying an electric or magnetic dipole. Being one of the simplest models featuring anisotropic interactions, they play a paramount role in liquid-state theories. From an applied science point of view, the exhibited strong response to external fields makes them suitable for applications in colloid science [1–4].

The strong anisotropy, associated to the long-range nature of the dipolar interaction, favours the formation of reversible chain-like structures at low temperatures T. This self-assembly process challenges the theoretical characterisation of such systems and raises doubts whether purely dipolar interactions can sustain a gas–liquid phase separation or not. In simple atomic and molecular fluids, where the attraction is due to van der Waals-like interactions, the condensation process leads to a separation between a low-density phase (gas) with high energy and high entropy and a high-density phase (liquid) with low energy and low entropy. A similar condensation mechanism for a dilute dipolar fluid was theorised by de Gennes and Pincus more than 40 years ago [5] for dipolar hard spheres (DHSs), i.e. for a system composed of point dipoles embedded in the centres of hard spheres. After observing that the spherically averaged interaction between two dipoles is attractive and akin to van der Waals molecular forces, they hinted at the existence of a gas–liquid critical point. Early simulations seemed to confirm this claim [6], but more recent and accurate numerical works suggest the absence of a critical phenomenon, at least in the region of the phase diagram where it was supposed to be located [7–10]. By analysing the structural properties of dipolar fluids at low temperatures and densities, these studies showed that the strongly anisotropic nature of the dipolar interactions plays a fundamental role in determining the thermodynamic behaviour of these systems. Indeed, at low temperatures, particles self-assemble in energetically favourable chain-like structures that were clearly found in the first computer simulation studies [7] and more recently in experiments on magnetic dipolar colloids [11]. As a result, the local ordering in a dipolar fluid is different from the isotropic phases of simple fluids and, depending on its extent, the linear aggregation in chains, being a unidimensional process, may suppress the phase separation [12,13]. Later on, the debate regarding the competition between condensation and self-assembly in DHS was enriched by a theoretical study [14] which predicted a topological phase transition featuring a re-entrant phase diagram. According to the theory developed by Tlusty and Safran (TS), the system phase separates in a low-density gas phase rich in chain ends, and in a high-density liquid phase rich in branched structures, i.e. in clusters made up of chains joined together by Y-shaped junctions. This peculiar phase separation is sustained rather than suppressed by self-assembly, and it depends on a delicate balance between the energetic costs associated to chain ends and three-way junctions. The topological phase transition has been recently observed in model of patchy particles designed to qualitatively reproduce the phenomenology of dipolar fluids [15–17].

Very recent simulation studies on the DHS model did not find any phase separation in the region where it was

*Corresponding author. Email: s.dussi@uu.nl

thought to be but, somewhat surprisingly, showed an unexpected abundance of rings at low densities ρ [10,18]. These ring structures arise from a subtle balance between the energy gained by having one additional bond and the entropy lost by reducing the volume accessible to chain ends. The main question about the existence of a gas–liquid critical point in the DHS model has no conclusive answer yet, but it is clear that any new theoretical modelling of the system must also consider rings, beside chains and branching points.

The DHS model is computationally very expensive because of the long-range nature of its interactions, of the very low temperature involved and because of the difficulty in equilibrating and relaxing the very long chain-like structures which are formed upon cooling [18]. For this reason, several models, which have the DHS model as a limiting case, have been introduced and investigated thoroughly [9,19]. Among them, charged dumbbells represent a key model to address some fundamental questions and to obtain a complete theoretical picture of dipolar fluids. Charged dumbbells are characterised by two oppositely charged spheres separated by a distance d. Charged dumbbells can be seen as a way of going from ionic-like systems, when d is very large, to dipolar systems, when $d \to 0$. Interestingly, the $d = 1$ case well reproduces the critical behaviour of the restricted primitive model (RPM) [20–22]. The two spheres can be either hard or soft, giving rise to charged hard dumbbells (CHD) or charged soft dumbbells (CSD), respectively. The dependence on d of the critical parameters in CHD models has been extensively studied by Camp and co-workers [20,23], who have provided a rough estimate for the location of the critical temperature of the DHS model by extrapolating these values at $d = 0$ [23]. Since a very recent study showed that no criticality appears in the vicinity of that temperature, what happens to the CHD model at very small separation d remains an open problem [10].

The behaviour of CSD models is complicated by the presence of one additional parameter (c) that controls the strength of the soft repulsion, usually modelled through a $\propto cr^{-12}$ potential. For a fixed T, varying c corresponds to change the effective size of the charged particles, altering the strength of the dipolar interaction at the (c-dependent) close contact value. Recently, the critical parameters of a CSD model have been computed for values of d spanning more than two order of magnitudes by Braun and Hentschke (BH) [21,24]. Small-elongation results are in agreement with the location of the critical parameters of the limiting dipolar soft sphere model calculated by the same authors [25]. To overcome the severe numerical difficulties, BH performed molecular dynamics simulations employing a reaction-field method in place of the more accurate Ewald sums. They rebuilt the equation of state of the model, extracting from the resulting van der Waals loop the coexistence points via the Maxwell equal area construction. Critical parameters (T_c, ρ_c) are then evaluated via fitting the coexistence curve with critical phenomena predictions based on the Ising universality class.

To quantify the effect of the reaction-field approximation and of the numerical methodology implemented by BH, we report here an independent evaluation of the critical parameters for selected values of the elongation d by means of successive umbrella sampling (SUS) Monte Carlo (MC) simulations where the long-range interactions are taken into account with the Ewald sums method. Our intent is twofold: first, we want to quantify the effect of long-range interactions by comparing our results with the reaction-field-computed results by BH. Second, we want to quantify the self-assembling processes taking place in the system as d decreases to shed light on the reasons why CSDs with very small elongation are hard to simulate.

The model and methodology are introduced in Section 2. Results on gas–liquid criticality and self-assembly analysis are described in Section 3, followed by a discussion in Section 4 where also guidelines for future investigations are suggested.

2. Model and simulation methods

A CSD consists of two oppositely charged soft spheres of diameter σ (set as the unit length) separated by a fixed distance d. The charge magnitude is $|q_-| = |q_+| = q$. Two dumbbells i, j interact through the following pair-potential:

$$U_{ij}(\{r_{i_a j_b}\}) = \sum_{a,b} \left(c \left(\frac{\sigma}{r_{i_a j_b}} \right)^{12} + \frac{q_a q_b}{4\pi\epsilon} \frac{\sigma}{r_{i_a j_b}} \right), \qquad (1)$$

where $a, b = +, -$ denote the charges of the dumbbells and $r_{i_a j_b} = |\mathbf{r}_{i_a} - \mathbf{r}_{j_b}|$ is the corresponding distance. Each CSD carries a dipole moment $|\boldsymbol{\mu}| = qd = 1$. This means that charges are progressively increased on decreasing d to maintain the particle dipole moment constant. The energy is expressed in units of $u = \mu^2/4\pi\epsilon\sigma^3$, the temperature T is given in dipolar units (k_B/u) and the density is defined by $\rho = \sigma^3 N/V$, where N is the number of dumbbells and V is the volume of the simulation box. In analogy with [21,24], we fixed $c = 4u$ and studied several values of d. Figure 1 shows the pair-interaction energy for the nose-to-tail and the anti-parallel side-by-side configurations as a function of d. The two curves cross at $d = d_c \simeq 0.70145$. Since nose-to-tail configurations are associated to chaining, one can use this crossover value as an estimate for the elongation at which this self-assembling process starts to occur.

Simulations were performed in a cubic box of side L (with L varying between 27 and 32, depending on d). Coulomb interactions are taken into account by Ewald sums with conducting boundary conditions [26]. We optimise the trigonometric calculations to provide an additional speed up.

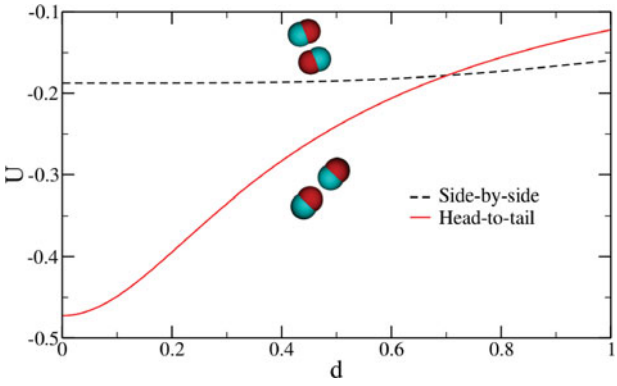

Figure 1. CSD pair interaction energy for the two lowest energy configurations (nose-to-tail and anti-parallel side-by-side) as a function of the dumbbell elongation for the selected model ($c = 4u$). The crossover between the two geometries takes place at $d = d_c \simeq 0.70145$.

We investigated the phase behaviour of CSDs by computing in the grand canonical (GC) ensemble the probability $P(\rho, E)$ at fixed T, V and activity z. To uniformly sample the density, we implemented the SUS method [27]. In this method, the density range is split into overlapping windows which are then explored in parallel by GCMC simulations. There is an additional constraint on the number of particles, which has to lie within the range assigned to each window. We used from 500 to 1000 windows, depending on the box size and on the density range. Each SUS window i is constrained to have a number of particles ranging from N_i to $N_i + 1$, and the overlap between two neighbouring windows is one, i.e. $N_{i+1} = N_i + 1$. The parallel nature of the SUS scheme allows to sensibly speed up simulations, since all the windows can be sampled at the same time.

Through standard histogram reweighting techniques [28], the simulation output $P(\rho, E)$, computed at fixed z, V, T, can be used to obtain the free-energy profiles at different z' and nearby T'. We estimate critical points by fitting $P(\rho, E)$ to the universal Ising distribution $P(M)$ by applying the Bruce–Wilding method [29], i.e. by considering $M \propto \rho + sE$, where s is a model-dependent constant whose value is determined by the fitting procedure.

Simulations of dipolar-like systems are intrinsically very challenging because of the chaining process that takes place in the low-temperature region. The resulting self-assembled aggregates are strongly bonded and long lived. Traditional MC moves are not efficient enough in breaking such structures and, in particular, the low acceptance rate of insertion and deletion moves represents the typical bottleneck of GCMC simulations carried out in this regime. To overcome this problem, we developed a new biased insertion/deletion move, in analogy with the procedure proposed for DHSs by Ganzenmüller *et al.* [9] and based on the idea of Caillol [8].

Due to the strong local electric field present in the proximity of large aggregates, a trial particle inserted with a random orientation would be very likely rejected. To improve insertion/deletion acceptance ratios, Ganzenmüller *et al.* introduced a biasing scheme for dipolar spheres that tends to orient the newly inserted particle dipole along the local field. Let **E** be the electric field at the trial insertion position **r**. The angle θ between the trial dipole and **E** is then randomly extracted from the biased distribution,

$$f(\cos(\theta)) = \frac{\beta\mu E \exp(\beta\mu E \cos(\theta))}{2\sinh(\beta\mu E)}. \qquad (2)$$

The previous formula follows from the angular average of the Boltzmann factor, which is analytically solvable for point-like dipoles (DHS or DSS models) but not for finite-sized ones (CHD or CSD models). To circumvent the problem, we introduce a new move consisting of two steps (Figure 2(a)): in the first stage we introduce a DSS oriented according to Equation (2), and then we transform it in a

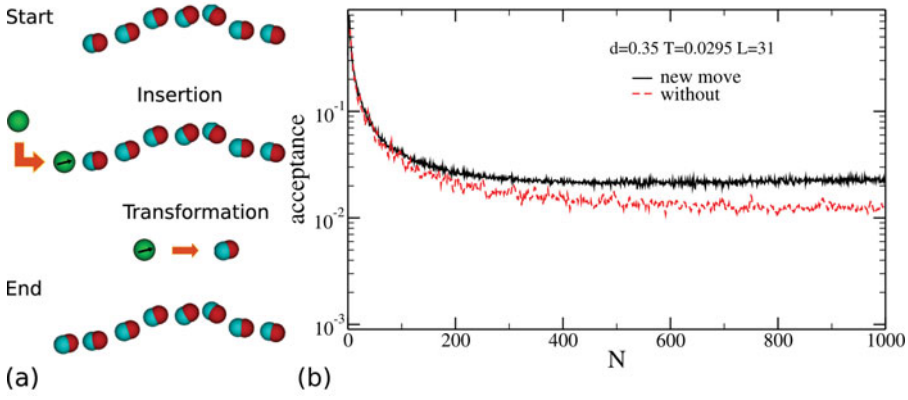

Figure 2. (a) Cartoon of the insertion–transformation MC move for CSD. (b) Acceptance rate for the insertion move for CSD with $d = 0.35$ at temperature $T = 0.0295$ and activity $z = 9.93 \times 10^{-5}$ with and without the new move introduced in the present work. The same behaviour is observed for the acceptance rate of the deletion move.

CSD with a probability given by

$$\text{acc}\,(\text{DSS} \rightarrow \text{CSD}) = \exp[-\beta(U_{\text{CSD}} - U_{\text{DSS}})], \qquad (3)$$

where $U_{DSS}(\mathbf{r}) = -\boldsymbol{\mu} \cdot \mathbf{E}(\mathbf{r}) + c/r^{12}$. Since the intermediate state of a DSS present in the system is to be avoided, the probability of accepting or rejecting a CSD insertion is given by the combination of the two steps and takes the following simple form (a standard GCMC criterion weighted with the local electric field):

$$\text{acc}(N \rightarrow N+1) = \min\left[1, \frac{1/2}{f(\cos(\theta))} \frac{zV \exp(-\beta U_{\text{CSD}})}{N+1}\right]. \qquad (4)$$

Analogously for the deletion move,

$$\text{acc}(N \rightarrow N-1) = \min\left[1, \frac{f(\cos(\theta))}{1/2} \frac{N \exp(\beta U_{\text{CSD}})}{zV}\right]. \qquad (5)$$

In general, the gain obtained using this move depends on the model parameters and on the simulated state point. Performance improvements are more evident at higher densities when the fluctuations of the local electric field are larger. Figure 2(b) shows the acceptance ratios of regular insertions and biased insertions for $d = 0.35$ and $T = 0.0295$ as a function of density.

We fix a ratio of 1:10 in the random choice between GC and roto-translational moves.

The structure is characterised through radial distribution functions, computed either on the centre of mass of the particles, $g(r)$ or on the charges position, $g_{+-}(r)$, and through the structure factor,

$$S(q) = \frac{1}{N}\left\langle \sum_{i=1}^{N}\sum_{j=1}^{N} \exp(i\mathbf{q} \cdot (\mathbf{r}_i - \mathbf{r}_j)) \right\rangle. \qquad (6)$$

At small d and low T, the dumbbells self-assemble into linear clusters. To investigate this process, we perform a standard cluster analysis by employing a mixed distance-energy bonding criterion: two dumbbells share a bond if the distance between their centres of mass is less than a cut-off distance r_{bond} and if their pair interaction energy is negative [10]. We fix r_{bond} in correspondence of the first minimum of $g(r)$. We then partition particles into clusters according to their topology.

- Chains are clusters of particles containing two ends (i.e. particles with just one bonded neighbour) connected by particles with only two bonded neighbours.
- Rings are clusters containing only doubly bonded particles.
- Branched structures contain at least one particle with more than two bonds.

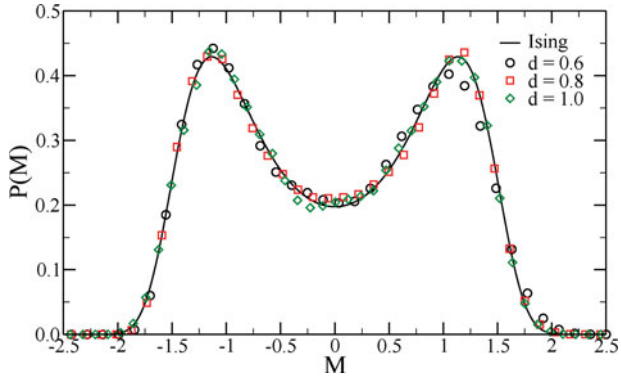

Figure 3. Best fits to the universal Ising distribution [30] for the simulated $P(\rho, E)$.

3. Results

3.1. Gas–liquid criticality

We first report on gas–liquid criticality by studying the density fluctuations distribution $P(\rho, E)$ obtained through SUS simulations of CSD with $c = 4$ and $d = 1, 0.8, 0.6,$ and 0.35. We investigate several temperatures to locate the critical points, starting with the estimates given by BH [21,24]. For $d \geq 0.6$, we find the expected gas–liquid separation and we are able to accurately locate the pseudo-critical points by fitting the obtained $P(\rho, E)$ to the universal Ising distribution. Figure 3 shows the best fits for these three investigated systems.

The resulting critical parameters T_c and ρ_c are plotted in Figure 4 and reported in Table 1 together with z_c and the fitting parameter s. The behaviour of both quantities as d decreases is qualitatively similar to the results presented by BH: T_c increases monotonically, while ρ_c exhibits a peak. Even though three points do not allow for a precise pinpointing of the peak position, we note that the position of the peak is compatible with the value of $d \simeq 0.70145$ at which the crossover between the nose-to-tail and the anti-parallel configuration as the energetically preferred geometry takes place. If this is the case, the maximum in ρ_c can act as an indicator to distinguish between the ionic-like and the dipolar-like regimes. From a quantitative point of view, T_c is really close to the values found by BH: for $d = 0.60$ the two values differ for less than 5%. A more significant difference is on ρ_c, since our results are sensibly larger (up to a factor of 2) than the ones computed by BH, signalling perhaps a significant effect of the way the long-range interactions are handled. We note that the values of the critical parameters and of s are in line with the corresponding values observed in the RPM model [31].

For $d = 0.35$, we are unable to clearly detect a critical point in the range of temperature studied (also indicated in Figure 4(a)). For this particular choice of d, we observe no criticality for $0.0295 \leq T \leq 0.035$. Figure 5 shows the resulting $P(\rho)$ at $T = 0.0295$, obtained summing

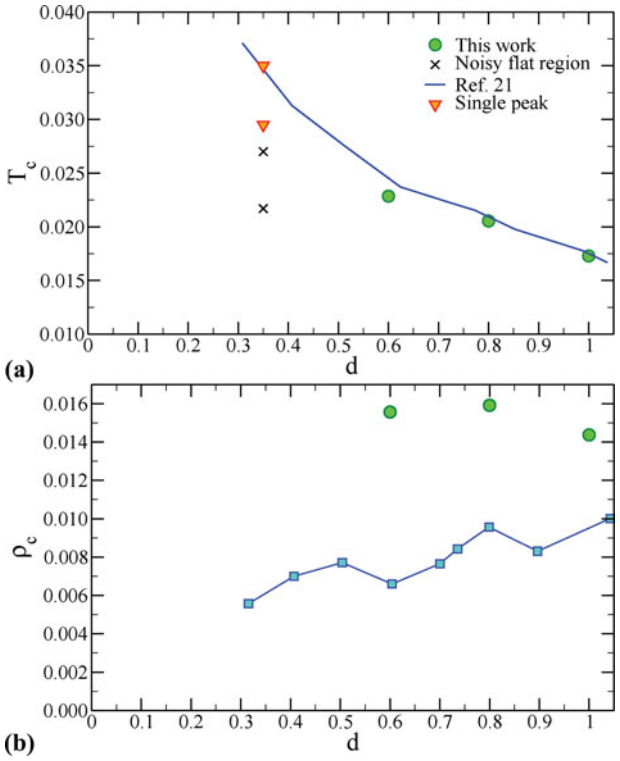

Figure 4. Pseudo-critical (a) temperatures and (b) densities for all the investigated models (circles). In (a) red triangles indicate a single-phase point and the crosses indicate the other investigated temperatures (see text). The blue line and symbols are taken from [21].

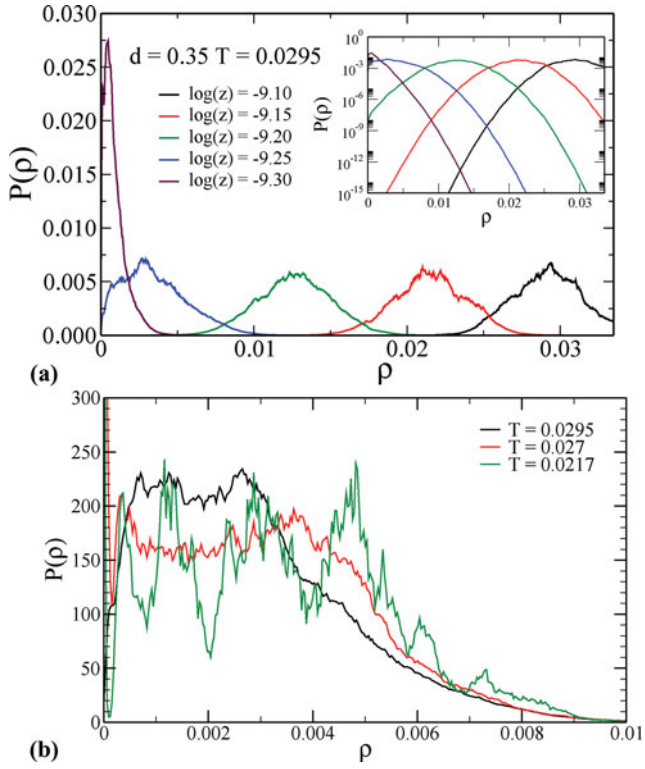

Figure 5. (a) $P(\rho)$ obtained through SUS simulations for CSD with $d = 0.35$ at $T = 0.0295$ in a box of side $L = 31$ and using histogram reweighting to span a large chemical potential interval. Inset: linear-log plot. (b) $P(\rho)$ for $d = 0.35$ for all the investigated temperatures, reweighted as to highlight the flat region present at low densities.

$P(\rho, E)$ over all possible E values, at different activities z: in the whole density range the distribution is always single peaked. As a reference, the BH pseudo-critical temperature for the same elongation is $T_c^{\mathrm{BH}} \approx 0.035$. As observed in both [23] (CHD) and [21], the critical temperature in charged dumbbell models is usually a monotonic function of d. By comparing with results for larger values of d, we expect $T_c(d = 0.35)$ to lie between $T \approx 0.023$ and $T = 0.0295$. Bearing this in mind, we carried out additional simulations at lower temperatures, but $P(\rho)$ never exhibits two clearly separated peaks. Figure 5(b) shows the low-density part of $P(\rho)$ for all investigated temperatures. At $T = 0.027$, a flat region appears at densities so low ($\rho \sim 0.002$) that we tentatively ascribe it to finite size effects. At these temperatures, the acceptance rate of GCMC moves drops off and the extensive clustering makes it really hard to properly sample the $P(\rho)$. Nevertheless we carried out a very long run at $T = 0.0217$, resulting in a still noisy $P(\rho)$, which shows no clear double-peaked structure and, once more, a flat region centred around $\rho \approx 0.003$.

The exact reason behind the absence of the critical phenomenon is not clear yet, but we can tentatively give two possible explanations.

(1) Finite size effects mask the phase transition, and simulations with sufficiently large boxes are basically infeasible with present-day computational tools. Hence the possibility to make progresses heavily depends on the ability to develop fast and reliable algorithms to speed up calculations.
(2) The critical point is moved to very low temperatures and densities by the self-assembling process, well below T at which equilibration can be reached. If this is the case, then the system is approaching a regime similar to what has been observed in a system of DHS plus a short-ranged attraction [9]: the system begins to self-assemble and to form stable, almost fully bonded aggregates which greatly reduce the driving force behind gas–liquid criticality. A small variation in the interaction results in a very large change in the critical temperature.

Table 1. Critical parameters for all the investigated models.

d	T_c	ρ_c	z_c	s
1.0	0.0172(8)	0.014(4)	3.479×10^{-4}	−7.35
0.8	0.0205(4)	0.015(9)	3.387×10^{-4}	−23.4
0.6	0.0228(5)	0.015(6)	1.925×10^{-4}	−19.8

The next sections support the latter hypothesis, but we cannot rule out the former.

3.2. Potential energy

In simple fluids, the gas–liquid phase separation is driven by the liquid having low energy and low entropy and the gas having high energy and high entropy. Since the large elongation $d = 1$ system is similar to the RPM, we expect a condensation-like transition to occur. Figure 6(a) shows the density dependence of the potential energy per particle U for different temperatures for the $d = 1$ system. As for simple fluids, the more dense the system, the lower the energy per particle. As shown in Figure 1, for $d > d_c$ it is energetically more convenient to form bonds via anti-parallel geometries, which lead to compact aggregates. Upon increasing the density, the number of neighbours per particle also increases. The energy difference between low and high densities is large enough to sustain a phase transition and the system can then separate in a low density, high energy gas and a high density, low energy liquid.

Reducing d below d_c drastically changes the potential energy per particle. Figure 6(b) shows the ρ-dependence of U/N for the $d = 0.35$ system for different temperatures. Strikingly, there is a very wide region in density for which U/N is a constant. This ρ region grows as the system is cooled down. A weak or no density dependence of the potential energy is a clear evidence of the onset of a self-assembly process and it has been also observed in low-T dipolar fluids [9,18,32]. The origin of this insensitivity on density can be traced back to the chaining process: since the nose-to-tail configuration is energetically preferred, the dumbbells tend to self-assemble into linear clusters, with each CSD having two neighbours, regardless of density. The energy per particle saturates in these structures and then, for a range of density that moves at lower and lower values as T decreases, the system is energetically less sensitive to a density variation because the only result in increasing the density is a larger number of such aggregates. The classical picture of a condensation does not fit any more.

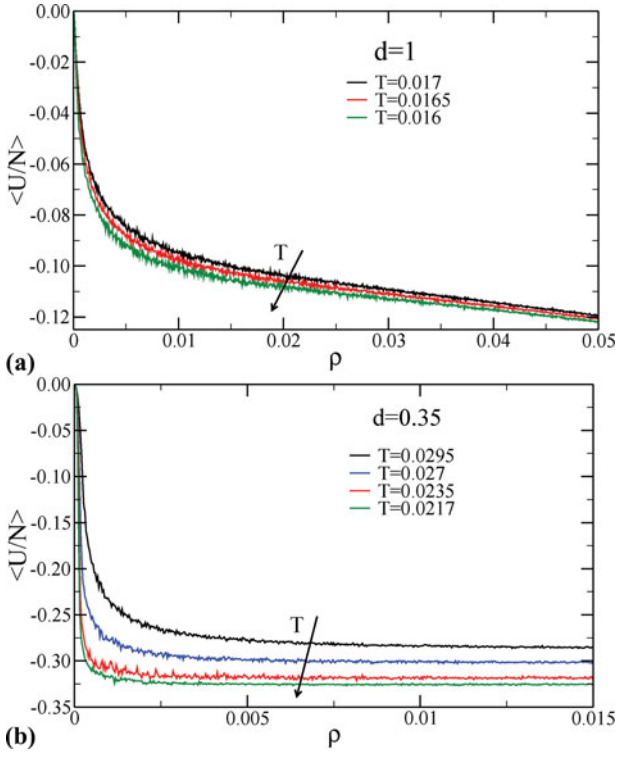

Figure 6. Potential energy per particle as a function of density for (a) $d = 1.0$ and (b) $d = 0.35$ for different temperatures.

3.3. Structural properties

In this section, we analyse the structure of CSD systems and we show how it changes when d decreases. As shown in Figure 1, as d decreases the system goes from being ionic-like to dipolar-like when d is small. In the ionic regime the system undergoes a phase separation and the condensation process involves compact clusters, similar to the RPM model [22]. A clear example of this mechanism can be seen in Figure 7(a), which shows a typical simulation snapshot for a $d = 1$ system in the liquid phase. The system is below the critical point, and we clearly observe dense aggregates containing side-by-side oriented pairs of dumbbells. The gas phase features similar orientations between neighbouring dumbbells, even though they aggregate into much smaller clusters.

For $d < d_c$, the head-to-tail configuration becomes more energetically favourable and the chaining process starts to take place. Upon cooling, chains become progressively longer and, if ρ increases, they merge together into branched structures which eventually form a percolating network. A further decrease in T can determine a kinetic arrest, giving rise to a reversible gel [33,34]. Figure 7(b) shows a typical simulation snapshot for $d = 0.35$ at 'high' density (higher than the expected critical density) and low temperature, where chain-like aggregates are interlinked in a

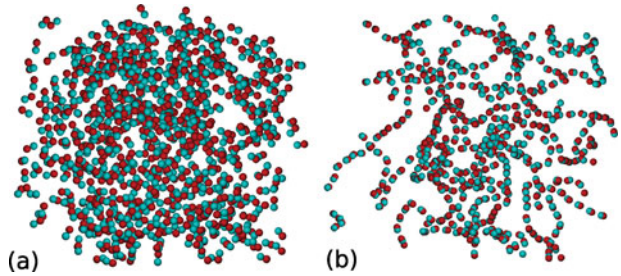

Figure 7. Typical simulation snapshots for (a) $d = 1$ and (b) $d = 0.35$ at high (liquid-like) density ($\rho = 0.0355$ and $\rho = 0.0138$, respectively).

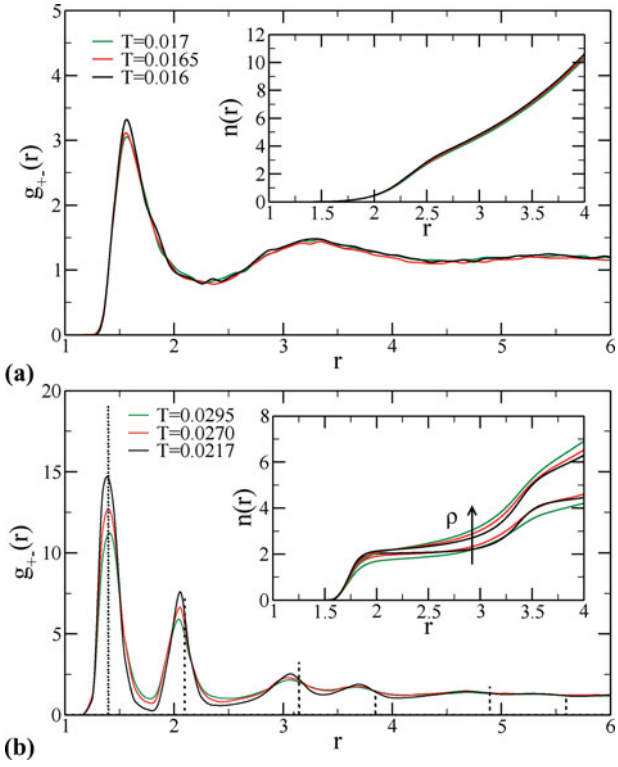

Figure 8. Charge-to-charge radial distribution function $g_{+-}(r)$ for (a) $d = 1$ and (b) $d = 0.35$ at $\rho = 0.0355$ and $\rho = 0.0138$, respectively. The dotted line in (b) is the $g_{+-}(r)$ (opportunely rescaled) for a linear ideal chain (see text for details). Insets: number of neighbours $n(r)$ for (a) $d = 1$ at $\rho = 0.0355$ and (b) $d = 0.35$ at $\rho = 0.0138$ and $\rho = 0.0016$ for different temperatures.

network structure. The figure strongly resembles snapshots of purely dipolar (i.e. $d \to 0$) systems [18,25].

To quantify the structural differences between CSDs of different inter-charges distance d, we study the charge–charge radial distribution function $g_{+-}(r)$.

Figure 8(a) shows $g_{+-}(r)$ for the $d = 1$ system in the liquid phase. The shape of the pair-correlation function resembles the ones found in simple liquids [35]: there are no distinct peaks for like-charges and unlike-charges and the maxima are quite broad and widely spaced.

The scenario for $d = 0.35$ is, once again, very different. In Figure 8(b), we plot $g_{+-}(r)$ for $d = 0.35$ at high density and for different T. The function is well structured at all T and, upon cooling the system, the peaks become higher and sharper and the minima deepen. The positions of the peaks clearly indicate a preference for the head-to-tail orientation. We also include the $g_{+-}(r)$ calculated for a perfect linear chain (dotted line). The good agreement between the peak positions and their relative heights confirms that chaining is the most relevant structural process in the system. The shift of the secondary peaks, which diminishes when T decreases, is due to the flexibility of the chains, whose decrease also controls the appearance of further peaks.

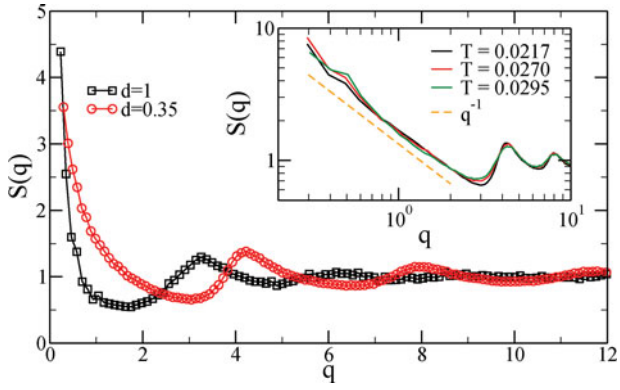

Figure 9. Structure factor $S(q)$ for $d = 0.35$ ($T = 0.0217$, $\rho = 0.00138$) and $d = 1$ ($T = 0.0016$, $\rho = 0.00355$). Inset: $S(q)$ T-dependence for $d = 0.35$. The orange dotted line is a power law with exponent -1.

To further investigate the local structure, we calculate the average number of neighbours within a sphere of radius r, which is linked to the dumbbells centre of mass $g(r)$ via

$$n(r) = 4\pi\rho \int_0^r r'^2 g(r')dr'. \tag{7}$$

The inset of Figure 8(a) shows $n(r)$ for $d = 1$. As expected, the function quickly loses its structure and begins to grow quadratically as $g(r)$ approaches 1. In the inset of Figure 8(b), we plot $n(r)$ for $d = 0.35$ for two densities and for different temperatures. We see in all cases a flat region starting from $r \simeq 1.75$, which becomes even flatter if T decreases. This plateau is another evidence of the chaining process, since the distance $r \simeq 1.75$ corresponds to the distance between two dumbbells in the head-to-tail configuration. The height of the plateau $n(r) \approx 2$ clearly indicates that the great majority of the dumbbells has only two neighbouring particles. At low density, this flat region extends to larger r, while increasing ρ determines a larger average number of neighbours, as expected.

The structural differences between the two regimes can also be observed through the structure factor $S(q)$, as shown in Figure 9. The structure factors of both systems grow at low q, but $d = 1$ $S(q)$ exhibits a much stronger increase due to the phase separation occurring in the system. By contrast, the growth of the low-q $S(q)$ of the $d = 0.35$ system, whose T-dependence is shown in the inset, is compatible with a power law with exponent 1, similar to what is found in purely dipolar systems [18,36].

3.4. *Self-assembly analysis*

In the previous section, we reported clear indications of the presence of linear aggregates in systems of CSD with small elongations. Indeed, the self-assembly process becomes more relevant upon reducing d. Here we want to

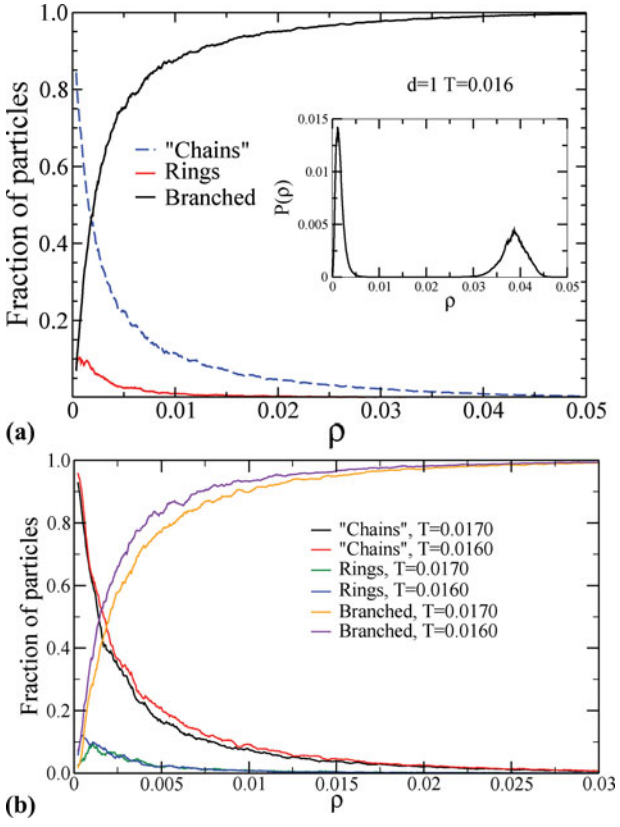

Figure 10. Self-assembly analysis for $d = 1$. (a) Fraction of particles in 'chains' (see text for definition), rings and branched clusters as a function of density at $T = 0.016$. Inset: corresponding $P(\rho)$. (b) Temperature dependence of the different structures.

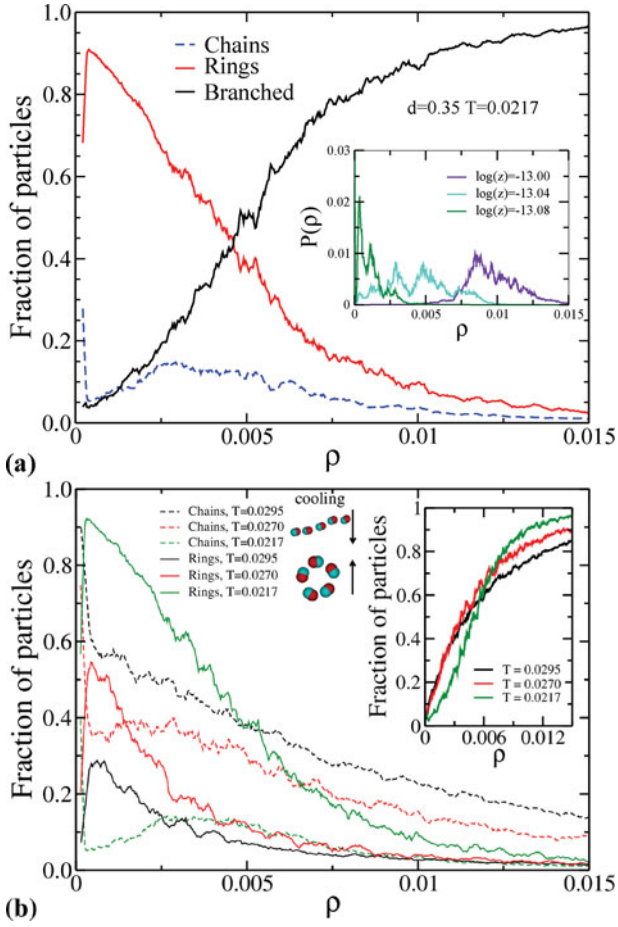

Figure 11. Self-assembly analysis for $d = 0.35$. (a) Fraction of particles in chains, rings and branched clusters as a function of density at $T = 0.0217$. Inset: corresponding $P(\rho)$ from SUS simulation. (b) Temperature dependence of rings and chains. Inset: T-dependence for branched clusters.

discriminate between different topological structures as anticipated in Section 2.

We used the bond criterion between two dumbbells introduced before and previously adopted for the DHS model [10]. The value of r_{bond} is based on the first minimum of the centre–centre $g(r)$, which depends very weakly on ρ.

In Figure 10(a) we report the fraction of particles in chains f_c, rings f_r and branched structures f_b as a function of the overall density for the $d = 1$ system at $T = 0.016 < T_c$. The SUS method indeed offers the possibility of sampling all the densities between the two coexisting ones, for which the system is phase separated and composed of a coexisting mixture of the two phases. First we note that, by our definition, monomers and dimers are defined as chains of one and two particles, respectively. For low densities, chains are the dominant topology of aggregates and their concentration drops off immediately as ρ increases. By analysing the cluster size distributions, we see that the majority of these 'chains' are indeed very small clusters made up of 1–5 dumbbells which, although satisfying our chain-like criterion, are more similar to ribbons than to chains [37]. Indeed, by comparing $P(\rho)$ at coexistence (inset), we see that these small clusters are what the gas phase is made of. The number of rings in the system is negligible. Figure 10(b) reports the T-dependence f_c, f_r and f_b for the same system. Upon cooling the system, f_c moves slightly towards lower densities as a result of the decrease in density of the gas phase. In addition, f_b undergoes a small shift to lower ρ. The number of rings does not change.

We then apply the same analysis to the $d = 0.35$ model, finding a completely different scenario. Figure 11(a) shows that, at $T = 0.0217$ (the lowest temperature investigated), the majority of the particles at low density belongs to ring structures and there are basically no more chains at any density. At high density branched structures are still dominant, as expected. The presence of rings has a tremendous impact on the equilibration time of the simulation: since every particle has two head-to-tail neighbours, the lifetime of a ring is incredibly long. The inset of Figure 11(a) shows $P(\rho)$ computed at different z after more than 2 months of simulations run on 100 CPU cores. On passing, we note that the first peak in the green curve ($z = \exp(-13.08)$)

is due to the fact that, for this model, rings of size ≈8 are favoured. Finally, in Figure 11(b) we report the temperature dependence of f_c, f_r and f_b. At the highest T, the density dependence resembles $d = 1$: chains are dominant at low density, branched clusters at high density and there are not many particles in rings in the whole density range. Upon cooling, f_b does not evolve considerably, while f_r starts to rise to the detriment of f_c. We see that already at $T = 0.027$ rings start to compete with chains, until they eventually suppress them almost completely at $T = 0.0217$. A similar abundance of rings was recently observed in the DHS model [18,38] and may be one of the reasons why no criticality seems to be present in the temperature range where it was predicted to occur.

The sudden increase in the fraction of particles in rings may imply that in the system there are not enough chains to sustain a topological phase transition as the one predicted by the TS theory. The question becomes how to determine the effect of the rings on the phase diagram of the system. A recent numerical study on two-dimensional patchy particles showed that rings can indeed suppress the liquid–gas phase separation [39].

4. Discussion and conclusions

In the present article, we consider a system composed of CSD, i.e. two oppositely charged spheres separated by a distance d. The same model was recently studied by BH by means of molecular dynamics simulations, with the long-range interactions being taken into account via a reaction-field method. We use the more rigorous, albeit more computationally expensive, Ewald sums method and through SUS MC simulations we investigate the dependence of the gas–liquid critical parameters on the dumbbell elongation d.

Our results confirm the criticality picture for elongated dumbbells ($d = 1, 0.8, 0.6$), although we find a difference in the critical values, especially for ρ_c. Reducing d to 0.35 we obtain a different scenario from the one presented by BH: the critical point (if present) shifts towards significantly lower T and ρ with respect to the critical parameters found by BH, in a region hardly accessible to simulations due to the very long lifetime of self-assembled aggregates. This discrepancy in the values of the critical parameters is ascribed to the different way of handling the long range interactions or to the different methodology to detect the phase separation, an issue that deserves a deeper investigation.

By analysing the average potential energy per particle, we see a striking difference between dumbbells with different elongations. Dumbbells with $d \gtrsim d_c$ tend to form compact clusters with a coordination number that grows upon increasing ρ. Cluster analysis shows that the low-density phase is composed of mostly monomers and very small clusters, while the high-density phase is a network of branched clusters, as expected for a condensation-like transition.

By contrast, $d \lesssim d_c$ values lead to the open nose-to-tail configuration being the most energetically favourable geometry. For a wide range of densities, each CSD has two neighbours and the average U/N does not increase upon increasing ρ. In this regime, as seen for other dipolar models, ring-shaped clusters start to form and they eventually become the most abundant aggregates at low densities. We link the absence of a phase separation to this massive presence of rings which, under certain conditions, can suppress phase separation entirely [39]. The possibility of fine tuning d to quantify the effect of self-assembly on criticality will be of invaluable importance for the understanding of the phase behaviour of dipolar fluids. Indeed, changing d changes both T_c and the temperatures at which ring formation becomes dominant. Finding a parameter combination, which features a reasonably high T_c and an abundance of rings at lower temperatures, will be key for the investigation of the interplay between self-assembly and phase separation.

Finally we note that the parameter c, which we have kept fixed throughout this work, tunes the ratio between the isotropic short-range soft repulsion and the anisotropic long-range dipolar interaction. It can then be used to control the thermodynamics and the dynamics of the system. BH [24] selected the value $c = 4$ (the same value studied in this article) to decrease the bond strength between particles and therefore allow for a faster equilibration of the system in molecular dynamics computer simulations. Indeed, the choice of c changes the curvature of the potential and its minimum. Smaller c values have been employed to investigate the dynamic properties of gel-like materials [32,33]. We note that the choice of c, which deeply affects the overall interaction potential, can also have strong effects on the formation of clusters and on the phase behaviour.

In conclusion, this work contributes to the long-standing question on the role of purely dipolar interactions on the thermodynamic properties of long-range interacting fluids. There is no definite answer yet, mainly because of the huge computational cost of simulating these systems. Overcoming the severe finite size effects, which appear at low temperatures, will require new specific algorithms and simulation techniques. From a theoretical point of view, the subtle balance between self-assembly and phase separation will have to be addressed by theories which also take into account ring structures.

Funding

We acknowledge support from ERC-PATCHYCOLLOIDS. S. Dussi acknowledges financial support from Nederlandse organisatie voor Wetenschappelijk Onderzoek (NWO).

References

[1] R.E. Rosensweig, Science **271**, 614 (1996).
[2] R.E. Rosensweig, *Ferrohydrodynamics* (Courier Dover Publications, New York, 1997).

[3] I. Szalai and S. Dietrich, J. Phys.: Condens. Matter **20** (20), 204122 (2008).
[4] B. Groh and S. Dietrich, Phys. Rev. Lett. **79**, 749 (1997).
[5] P.G. de Gennes and P.A. Pincus, Physik der Kondensierten Materie **11**, 189 (1970).
[6] K. Ng, J.P. Valleau, G.M. Torrie, and G.N. Patey, Mol. Phys. **38**, 781 (1979).
[7] J.J. Weis and D. Levesque, Phys. Rev. Lett. **71**, 2729 (1993).
[8] J.M. Caillol, J. Chem. Phys. **98** (12), 9835–9849 (1993).
[9] G. Ganzenmüller, G.N. Patey, and P.J. Camp, Mol. Phys. **107**, 403 (2009).
[10] L. Rovigatti, J. Russo, and F. Sciortino, Phys. Rev. Lett. **107**, 237801 (2011).
[11] M. Klokkenburg, R.P.A. Dullens, W.K. Kegel, B.H. Erné, and A.P. Philipse, Phys. Rev. Lett. **96**, 037203 (2006).
[12] R.P. Sear, Phys. Rev. Lett. **76**, 2310 (1996).
[13] R. van Roij, Phys. Rev. Lett. **76** (18), 3348–3351 (1996).
[14] T. Tlusty and S.A. Safran, Science **290**, 1328 (2000).
[15] J. Russo, J.M. Tavares, P.I.C. Teixeira, M.M. Telo da Gama, and F. Sciortino, J. Chem. Phys. **135**, 034501 (2011).
[16] J. Russo, J.M. Tavares, P.I.C. Teixeira, M.M. Telo da Gama, and F. Sciortino, Phys. Rev. Lett. **106**, 085703 (2011).
[17] N.G. Almarza, J.M. Tavares, E.G. Noya, and M.M.T. da Gama, J. Chem. Phys. **137** (24), 244902 (2012).
[18] L. Rovigatti, J. Russo, and F. Sciortino, Soft Matter **8**, 6310 (2012).
[19] N.G. Almarza, E. Lomba, C. Martín, and A. Gallardo, J. Chem. Phys. **129** (23), 234504 (2008).
[20] C.D. Daub, G.N. Patey, and P.J. Camp, J. Chem. Phys. **119** (15), 7952–7956 (2003).
[21] H. Braun and R. Hentschke, Phys. Rev. E **87**, 012311 (2013).
[22] A.Z. Panagiotopoulos, J. Phys.: Condens. Matter **17** (45), 53205–53213 (2005).
[23] G. Ganzenmüller and P.J. Camp, J. Chem. Phys. **126**, 191104 (2007).
[24] H. Braun and R. Hentschke, Phys. Rev. E **80**, 041501 (2009).
[25] R. Jia, H. Braun, and R. Hentschke, Phys. Rev. E **82** (6), 062501 (2010).
[26] B. Smit and D. Frenkel, *Understanding Molecular Simulations* (Academic, New York, 1996).
[27] P. Virnau and M. Müller, J. Chem. Phys. **120** (23), 10925–10930 (2004).
[28] A.M. Ferrenberg and R.H. Swendsen, Phys. Rev. Lett. **63** (12), 1195–1198 (1989).
[29] N.B. Wilding and A.D. Bruce, J. Phys.: Condens. Matter **4** (12), 3087–3108 (1992).
[30] M.M. Tsypin and H.W.J. Blöte, Phys. Rev. E **62**, 73 (2000).
[31] G. Orkoulas and A.Z. Panagiotopoulos, J. Chem. Phys. **110** (3), 1581–1590 (1999).
[32] M.A. Floriano, E. Caponetti, and A.Z. Panagiotopoulos, Langmuir **15** (9), 3143–3151 (1999).
[33] R. Blaak, M.A. Miller, and J.P. Hansen, Europhys. Lett. **78**, 26002 (2007).
[34] M.A. Miller, R. Blaak, C.N. Lumb, and J.P. Hansen, J. Chem. Phys. **130** (11), 114507 (2009).
[35] J.P. Hansen and I.R. McDonald, *Theory of Simple Liquids*, 3rd ed. (Academic Press, New York, 2006).
[36] P.J. Camp and G.N. Patey, Phys. Rev. E **62**, 5403 (2000).
[37] J. Yan, K. Chaudhary, S.C. Bae, J.A. Lewis, and S. Granick, Nat. Commun. **4**, 1516 (2013).
[38] S. Kantorovich, A.O. Ivanov, L. Rovigatti, J.M. Tavares, and F. Sciortino, Phys. Rev. Lett. **110**, 148306 (2013).
[39] N.G. Almarza, Phys. Rev. E **86**, 030101 (2012).